Production of T_{cc}^{+} exotic state in the $\gamma p \to D^{+}\bar{T}_{cc}^{-}\Lambda_c^{+}$ reaction

Yin Huang[1,2] Hong Qiang Zhu[3,*] Li-Sheng Geng,[4,†] and Rong Wang[5,6]

[1]*School of Physical Science and Technology, Southwest Jiaotong University, Chengdu 610031, China*
[2]*Asia Pacific Center for Theoretical Physics, Pohang University of Science and Technology, Pohang 37673, Gyeongsangbuk-do, South Korea*
[3]*College of Physics and Electronic Engineering, Chongqing Normal University, Chongqing 401331, China*
[4]*School of Physics and Nuclear Energy Engineering, Beihang University, Beijing 100191, China*
[5]*Institute of Modern Physics, Chinese Academy of Sciences, Lanzhou 730000, China*
[6]*University of Chinese Academy of Sciences, Beijing 100049, China*

(Received 1 September 2021; accepted 10 November 2021; published 14 December 2021)

Stimulated by the recent LHCb observation of a new exotic charged structure T_{cc}^{+}, we propose to use the central diffractive mechanism existing in the $\gamma p \to D^{+}\bar{T}_{cc}^{-}\Lambda_c^{+}$ ($\bar{T}_{cc}^{-}$ is the antiparticle of T_{cc}^{+}) reaction to produce T_{cc}^{+}. Our theoretical approach is based on the chiral unitary theory where the T_{cc}^{+} resonance is dynamically generated. With the coupling constant of the T_{cc}^{+} to DD^{*} channel obtained from chiral unitary theory, the total cross sections of the $\gamma p \to D^{+}\bar{T}_{cc}^{-}\Lambda_c^{+}$ reaction are evaluated. Our study indicates that the cross section for $\gamma p \to D^{+}\bar{T}_{cc}^{-}\Lambda_c^{+}$ reaction is on the order of 1.0 pb, which is accessible at the proposed the Electron-Ion Collider in China [Front. Phys. (Beijing) **16**, 64701 (2021)] or the U.S. [Eur. Phys. J. A **52**, 268 (2016)] due to the higher luminosity. If measured and confirmed in the future experiments, the predicted total cross sections can be used to verify the (molecular) nature of the T_{cc}^{+}.

DOI: 10.1103/PhysRevD.104.116008

I. INTRODUCTION

Exotic hadrons [1] have been the focus of theoretical and experimental interest since they have an internal structure more complex than the simple $\bar{q}q$ configuration for mesons or qqq configuration for baryons in the traditional constituent quark models [2]. In particular, understanding their production mechanism and using it as a probe to the structure of the hadrons are among the most active research fields in particle and nuclear physics [3]. The challenge is to understand the nonperturbative transition from high-energy $e^{+}e^{-}$, photon-hadron, and hadron-hadron collisions to physical exotic states. In this work, we report a central diffractive contribution existing in the $\gamma p \to D^{+}\bar{T}_{cc}^{-}\Lambda_c^{+}$ reaction to understand the newly observed doubly charmed meson T_{cc}^{+}.

The charmed meson T_{cc}^{+} with $I(J^P) = 0(1^{+})$ was first observed by the LHCb Collaboration in the $D^0D^0\pi^{+}$ invariant mass spectrum [4]. Its mass and width are measured to be

$$m = 3875.09\ \text{MeV} + \delta m,$$
$$\Gamma = 410 \pm 165 \pm 43^{+18.0}_{-38}\ \text{keV}, \tag{1}$$

respectively, where the δm is binding energy and measured to be equal to $\delta m = -273 \pm 61 \pm 5^{+11}_{-14}$ keV. From the $D^0D^0\pi^{+}$ decay mode, the new structure T_{cc}^{+} contains at least four valence quarks. Because the quark components of D^0 and π^{+} mesons are $c\bar{u}$ and $u\bar{d}$, respectively, the T_{cc}^{+} is another new candidate of a tetraquark state with double-charm quarks following the previous observation of the doubly charmed baryon state $\Xi_{cc}^{++}(3621)$ [5].

In fact, there were already a few theoretical studies on the existence of such a state before discovery. A loosely $D^{(*)}D^{(*)}$ bound state with a binding energy of 0.47–42.82 MeV was predicted by taking into account the coupled channel effect, and the isospin (spin parity) of the T_{cc}^{+} state was suggested to be $I(J^P) = 0(1^{+})$ [6]. The mass spectrum of the doubly charmed meson state T_{cc}^{+} around 3873 MeV was investigated in the one-boson-exchange model [7], which can be associated with the LHCb observation [4,8]. In Refs. [9,10], a doubly charmed compact tetraquark state above the DD^{*} mass threshold was predicted by considering the heavy quark symmetry. The axial-vector tetraquark state of $cc\bar{u}\bar{d}$ was studied using the QCD sum rule method [11]. Exotic mesons $J^P = 0^{\pm}$ and $1^{\pm}$ with a general content $cc\bar{q}\bar{q}'$ in the same approach were investigated in Ref. [12]. The axial-vector state $cc\bar{u}\bar{d}$ was modeled as a hadronic molecule of D^0D^{*+} [13].

*20132013@cqnu.edu.cn
†lisheng.geng@buaa.edu.cn

Following the discovery of the T_{cc}^+, several theoretical studies have been performed. The mass and current coupling of the newly observed doubly charmed four-quark state T_{cc}^+ is calculated in the QCD two-point sum rule method with the conclusion that the T_{cc}^+ can be assigned as an axial-vector tetraquark [14]. Since the mass of T_{cc}^+ is just 273 keV below the $D^{*+}D^0$ threshold, it can be naturally understood as a DD^* molecule [15–21]. From Refs. [14–21], it seems that the T_{cc}^+ can not only be explained as a compact tetraquark state but also as a molecular state. Moreover, the parameters, such as the mass $\delta m_{\text{pole}} = -340 \pm 40^{+4}_{-0}$ keV and width $\Gamma_{\text{pole}} = 48 \pm 2^{+0}_{-14}$ keV given in Ref. [8] are different from the mass $\delta m = -273 \pm 61 \pm 5^{+11}_{-14}$ keV and width $\Gamma = 410 \pm 165 \pm 43^{+18.0}_{-38}$ keV given in Ref. [4]. Because the two sets of parameters are obtained from different fits to the inclusive cross sections, it is not yet clear which set of parameters one should trust. Theoretical and experimental studies of the production mechanism of the T_{cc}^+ state can provide crucial information in better understanding its nature.

In this work, we report on a theoretical study of $\bar{T}_{cc}^-$ in the $\gamma p \to D^+\bar{T}_{cc}^-\Lambda_c^+$ reaction employing the central diffractive mechanism, which has been widely employed to investigate the production of hadrons in pp collisions [22–25]. However, it was not studied in too much detail in photon-hadron reactions either experimentally or theoretically. This is because, at not too high energies, the hadrons in the final state contribute negligibly to central diffractive productions compared with other processes [25]. High-energy photon beams are available at the Electron-Ion Collider in China (EICC) [26] or the U.S. (US-EIC) [27], which provide another alternative to study the $\gamma p \to D^+\bar{T}_{cc}^-\Lambda_c^+$ reaction by considering the central diffractive mechanism. The contributions for the $\gamma p \to D^+\bar{T}_{cc}^-\Lambda_c^+$ reaction from other channels, such as $s-$ and $u-$ channels, are ignored because the $s-$ and $u-$ channels, which involve the creation of two additional $\bar{c}c$ quark pairs in the photon-induced production, are usually strongly suppressed. Thus, the central diffractive mechanism provides the dominant contribution in the $\gamma p \to D^+\bar{T}_{cc}^-\Lambda_c^+$ reaction and is a new tool to reveal the nature of the T_{cc}^+.

II. THEORETICAL FORMALISM

First we explain the central diffractive mechanism responsible for the $\gamma p \to D^+\bar{T}_{cc}^-\Lambda_c^+$ reaction. Similar to the central diffractive mechanism in pp collisions, at higher energies free $\bar{D}^*\bar{D}$ production is dominant, while at lower energies the $\bar{D}^*$ and $\bar{D}$ interact strongly and produce $\bar{T}_{cc}^-$. The tree-level Feynman diagrams are depicted in Fig. 1.

To compute the diagrams shown in Fig. 1, we need the effective Lagrangian densities for the relevant interaction vertices. As mentioned in Refs. [15–21], the T_{cc}^+ resonance can be identified as an S-wave D^*D molecule. Because the

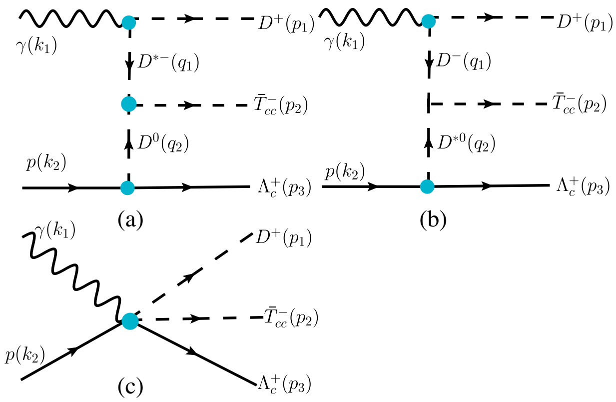

FIG. 1. Central diffractive mechanism responsible for the production of $\bar{T}_{cc}^-$ in the γp collision where $\bar{T}_{cc}^-$ is treated as a $D^{*-}\bar{D}^0$ hadronic molecule. The definitions of the kinematics $(p_1, p_2, p_3, k_1, k_2, q_1, q_2)$ are also shown. The $\bar{T}_{cc}^-$ represents the antiparticle of T_{cc}^+.

lowest angular momentum gives the dominant contribution in the near-threshold region, a constant amplitude can be used for the S-wave vertex of the $T_{cc}D^*D$. Thus, the Lagrangian density for the S-wave coupling of T_{cc}^+ with its components can be written down as [28,29]

$$\mathcal{L}_{T_{cc}D^*D} = g_{T_{cc}} T_{cc}^{\mu\dagger} D_\mu^* D, \tag{2}$$

where $g_{T_{cc}}$ is the coupling constant. Using exactly the same strategy as in Ref. [18], a state barely bound that can be associated with the current T_{cc} [4,8] is found.

The couplings of the bound state to the coupled channels $D^{*+}D^0$ (channel 1) and $D^{*0}D^+$ (channel 2) can be obtained from the residue of the scattering amplitude at the pole position z_R, which reads

$$T_{ij} = \frac{g_{ii}g_{jj}}{\sqrt{s} - Z_R}, \tag{3}$$

where g_{ii} is the coupling of the state to the ith channel. The coupling constants are found to be

$$g_{T_{cc}D^{*+}D^0} = 3.67 \text{ GeV}, \qquad g_{T_{cc}D^{*0}D^+} = -3.92 \text{ GeV}, \tag{4}$$

and, as we can see, they are basically opposite to each other, indicating that the T_{cc}^+ is a quite good $I = 0$ bound state. Detailed calculations and discussions can be found in Ref. [18].

In addition to the vertices described by Eq. (2), the following effective Lagrangians [30,31] are needed to evaluate the Feynman diagrams shown in Fig. 1. Because we study the production rate of the T_{cc}^+ in the near-threshold region, it is sufficient to consider effective Lagrangians that have the smallest number of derivatives, which are given as follows [30,31]:

$$\mathcal{L}_{\Lambda_c ND^*} = g_{D^*N\Lambda_c} \bar{\Lambda}_c \gamma^\mu N D_\mu^* + \text{H.c.}, \tag{5}$$

$$\mathcal{L}_{\Lambda_c ND} = ig_{DN\Lambda_c}\bar{\Lambda}_c\gamma_5 ND + \text{H.c.}, \tag{6}$$

$$\mathcal{L}_{\gamma DD^*} = g_{\gamma DD^*}\epsilon_{\mu\nu\alpha\beta}(\partial^\mu \mathcal{A}^\nu)(\partial^\alpha D^{*\beta})D + \text{H.c.}, \tag{7}$$

$$\mathcal{L}_{\gamma DD} = ie\mathcal{A}_\mu(D^+\partial^\mu D^- - \partial^\mu D^+ D^-), \tag{8}$$

where $\mathcal{A}^\mu$, D, $D^{*\mu}$, N, and Λ_c are the photon, D meson, D^* meson, nucleon, and Λ_c^+ baryon fields, respectively. $e = \sqrt{4\pi\alpha}$ with α being the fine-structure constant. Coupling constants $g_{DN\Lambda_c} = -13.98$ and $g_{D^*N\Lambda_c} = -5.20$ [32,33] are obtained from SU(4) invariant Lagrangians [34] in terms of $g_{\pi NN} = 13.45$ and $g_{\rho NN} = 6$. The coupling constant $g_{D^*D\gamma}$ is determined by the radiative decay widths of D^*,

$$\Gamma_{D^{*\pm}\to D^\pm\gamma} = \frac{g_{D^*D\gamma}^2(m_{D^*}^2 - m_D^2)^2}{48\pi m_{D^*}^2}|\vec{p}_D^{\text{c.m.}}|, \tag{9}$$

where $\vec{p}_D^{\text{c.m.}}$. is the three-vector momentum of the D in the D^* meson rest frame. With $m_{D^*} = 2.01$ GeV, $m_D = 1.87$ GeV, and $\Gamma_{D^{*\pm}\to D^\pm\gamma} = 0.979$–$1.704$ keV [1], one obtains $g_{D^*D\gamma} = 0.173$–$0.228\ \text{GeV}^{-1}$. According to the lattice QCD and QCD sum rule calculations [35,36], the minus sign for $g_{D^*D\gamma}$ is adopted, and the minus sign for $g_{D^*D\gamma}$ is in relation to the dimensionless form factor $F_{u,d}(0)$ of the D meson [35,36].

In evaluating the scattering amplitudes of the $\gamma p \to D^+\bar{T}_{cc}^-\Lambda_c^+$ reaction, we need to include form factors because hadrons are not pointlike particles. For the exchanged D and D^* mesons, we apply a widely used monopole form factor, which is written as

$$\mathcal{F}_i = \frac{\Lambda_i^2 - m_i^2}{\Lambda_i^2 - q_i^2} \qquad i = D, D^*, \tag{10}$$

where q_i and m_i are the four-momentum and the mass of the exchanged $D^{(*)}$ meson, respectively. The Λ_i is the hard cutoff, and it can be directly related to the hadron size. Empirically, the cutoff parameter Λ_i should be at least a few hundred MeV larger than the mass of the exchanged hadron. Hence, the $\Lambda_i = m_i + \alpha\Lambda_{\text{QCD}}$ and the QCD energy scale $\Lambda_{\text{QCD}} = 220$ MeV is adopted in this work. The α reflects the nonperturbative property of QCD at the low-energy scale and it can only be determined from experimental data. In the following, it will be taken as a parameter and discussed later.

The propagator for the D meson is written as

$$G_D(q) = \frac{i}{q^2 - m_D^2}. \tag{11}$$

For the D^* exchange, we take the propagator as

$$G_{D^*}^{\mu\nu}(q) = \frac{i(-g^{\mu\nu} + q^\mu q^\nu/m_{D^*}^2)}{q^2 - m_{D^*}^2}, \tag{12}$$

where μ and ν are the polarization indices of D^*.

With all these ingredients, the invariant scattering amplitude of the $\gamma p \to D^+\bar{T}_{cc}^-\Lambda_c^+$ reaction demonstrated in Fig. 1 can be constructed as

$$\begin{aligned} -i\mathcal{M}_j = {} & \bar{u}(p_3, \lambda_{\Lambda_c^+})\mathcal{W}_j^{\mu\nu}u(k_2, \lambda_p) \\ & \times \epsilon_\nu(k_1, \lambda_\gamma)\epsilon_\mu^*(p_2, \lambda_{T_{cc}^-}), \end{aligned} \tag{13}$$

where j denotes diagrams a, b of Fig. 1 or a contact term contribution that will be explained below, while u and ϵ are the Dirac spinor and polarization vector, respectively. $\lambda_{\Lambda_c^+}$, λ_p, $\lambda_{T_{cc}^-}$, and λ_γ are the helicities for the Λ_c^+, the proton, the $\bar{T}_{cc}^-$, and the photon, respectively.

Then the reduced amplitudes $\mathcal{W}_j^{\mu\nu}$ read as

$$\begin{aligned} \mathcal{W}_a^{\mu\nu} = {} & g_a\gamma_5\epsilon_{\alpha\nu\beta\rho}k_1^\alpha q_1^\beta \\ & \times \frac{-g^{\mu\rho} + q_1^\mu q_1^\rho/m_{D^{*-}}^2}{q_1^2 - m_{D^{*-}}^2 + im_{D^{*-}}\Gamma_{D^{*-}}}\frac{\mathcal{F}_a}{q_2^2 - m_{\bar{D}^0}^2}, \end{aligned} \tag{14}$$

$$\begin{aligned} \mathcal{W}_b^{\mu\nu} = {} & g_b\gamma_\rho(q_1^\nu - p_1^\nu) \\ & \times \frac{-g^{\mu\rho} + q_2^\mu q_2^\rho/m_{\bar{D}^{*0}}^2}{q_2^2 - m_{\bar{D}^{*0}}^2 + im_{\bar{D}^{*0}}\Gamma_{\bar{D}^{*0}}}\frac{\mathcal{F}_b}{q_1^2 - m_{D^-}^2}, \end{aligned} \tag{15}$$

where $g_a = -g_{D^*D\gamma}g_{DN\Lambda_c}g_{\bar{T}_{cc}}$, $g_b = -ieg_{D^*N\Lambda_c}g_{\bar{T}_{cc}}$, $\mathcal{F}_a = \mathcal{F}_{\bar{D}^0}\mathcal{F}_{D^{*-}}$, and $\mathcal{F}_b = \mathcal{F}_{\bar{D}^{*0}}\mathcal{F}_{D^-}$. The charge of the hadron is in units of $e = \sqrt{4\pi\alpha}$ with α being the fine-structure constant. $\epsilon^{\mu\nu\alpha\beta}$ is the Levi-Civita tensor with $\epsilon^{0123} = 1$. Here we take $\Gamma_{D^*,\bar{D}^*} = 0$ MeV for the D^* and the $\bar{D}^*$ states because their widths are on the order of tens of keV.

Obviously, the amplitude cannot satisfy gauge invariance only with diagrams included in Figs. 1(a) and 1(b). To ensure gauge invariance of the total amplitude, the contact diagram shown in Fig. 1(c) must be included. Therefore, we introduce a generalized contact term as follows:

$$\mathcal{W}_c^{\mu\nu} = 2g_b(-\gamma_\mu + \mathcal{H}q_2^\mu)\frac{(k_1^\nu - p_1^\nu)}{q_2^2 - m_{\bar{D}^{*0}}^2}\frac{\mathcal{F}_b}{q_1^2 - m_{D^-}^2} \tag{16}$$

to satisfy

$$k_1^\nu\left(\sum_{j=a,b,c}\mathcal{M}_{\nu,j}\right) = 0, \tag{17}$$

where $\mathcal{H} = (m_p - m_{\Lambda_c^+})/m_{\bar{D}^{*0}}^2$, with m_p and $m_{\Lambda_c^+}$ as the masses of proton and Λ_c^+, respectively.

The differential cross section in the c.m. frame for the $\gamma p \to D^+\bar{T}_{cc}^-\Lambda_c^+$ reaction reads

$$
\begin{aligned}
&d\sigma(\gamma p \to \Lambda_c^+ D^+ \bar{T}_{cc}^-) \\
&= \frac{m_p}{2(k_1 \cdot k_2)} \sum_{s_i, s_f} |-i\mathcal{M}(\gamma p \to \Lambda_c^+ D^+ \bar{T}_{cc}^-)|^2 \\
&\times \frac{d^3\vec{p}_1}{2E_1} \frac{d^3\vec{p}_2}{2E_2} \frac{m_{\Lambda_c^+} d^3\vec{p}_2}{E_2} \delta^4(k_1 + k_2 - p_1 - p_2 - p_3), \quad (18)
\end{aligned}
$$

where E_1, E_2, and E_3 stand for the energies of D^+, $\bar{T}_{cc}^-$, and final Λ_c^+, respectively, and $\mathcal{M} = \mathcal{M}_a + \mathcal{M}_b + \mathcal{M}_c$ is total scattering amplitude of the $\gamma p \to D^+ \bar{T}_{cc}^- \Lambda_c^+$ reaction.

III. RESULTS AND DISCUSSIONS

The mass of T_{cc}^+ is slightly below the D^*D threshold. It is natural to treat it as a D^*D molecular state, dynamically generated from the interaction of the coupled channels $D^{*+}D^0$ and $D^{*0}D^+$ in the isospin $I = 0$ sector. Considering the new structure T_{cc}^+ as a molecular state, its production in the $\gamma p \to D^+ \bar{T}_{cc}^- \Lambda_c^+$ reaction is evaluated via the central diffractive mechanism and the contact term to ensure the gauge invariance. However, the contributions for the $\gamma p \to D^+ \bar{T}_{cc}^- \Lambda_c^+$ reaction from other channels, such as $s-$ and $u-$ channels, are ignored because the $s-$ and $u-$ channels involve the creation of two additional $\bar{c}c$ quark pairs in the photon-induced production and are strongly suppressed.

To make a reliable prediction for the cross section of the $\gamma p \to D^+ \bar{T}_{cc}^- \Lambda_c^+$ reaction, the only issue we need to clarify is the value of α of the form factors. The α reflects the nonperturbative property of QCD at low-energy scales and could not be determined from first principles. It is usually determined from experimental branching ratios. We noticed studies of α have been performed by comparison with experimental data [37,38], whose procedures are illustrated in Ref. [39]. In this work, we adopt $a = 1.5$ or 1.7 because this value is determined from the experimental data [37,38] with the same D and D^* form factors adopted in the work of Ref. [39].

With the formalism and ingredients given above, the total cross section as a function of the c.m. energy $\sqrt{s}$ $[s = (k_1 + k_2)^2]$ for the $\gamma p \to D^+ \bar{T}_{cc}^- \Lambda_c^+$ reaction can be easily obtained. The theoretical results obtained with a cutoff $\alpha = 1.5$ or 1.7 for the c.m. energy from near threshold up to 12.0 GeV are shown in Fig. 2. The total cross section increases with α in the discussed cutoff range but the dependence is relatively weak. Taking $\sqrt{s} = 10$ GeV and $\Gamma_{D^{*\pm} \to D^{\pm}\gamma} = 1.334$ keV as an example, the increase of the cutoff parameter from 1.5 to 1.7 results in an increase of the cross section runs from 0.262 to 0.426 pb.

Figure 2 also shows that the total cross section increases sharply near the threshold. At higher energies, the cross section increases continuously but relatively slowly compared with that near threshold. The cross section increases sharply near the threshold can be easily understood, since at that energy, the invariant mass of the $D^+ \bar{T}_{cc}^- \Lambda_c^+$ system will reach and pass by 8031.21 MeV, which is the sum of the D^+, $\bar{T}_{cc}^-$, and Λ_c^+ masses. Then, the phase space opens and leads to a sharp increase of the cross section near the threshold. The phase space as a function of the c.m. energy $\sqrt{s}$ is shown in Fig. 3.

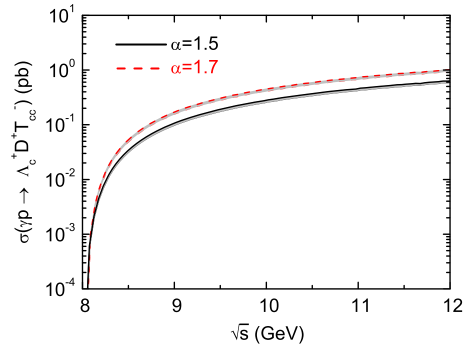

FIG. 2. Total cross section for the $\gamma p \to D^+ \bar{T}_{cc}^- \Lambda_c^+$ reaction with $\Gamma_{D^{*\pm} \to D^{\pm}\gamma} = 0.979$–$1.704$ keV [1] as a function of $\sqrt{s}$.

The difference between the cross section predicted with $\alpha = 1.5$ and that predicted with $\alpha = 1.7$ becomes larger as the energy increases. The total cross section is about 0.7 and 0.4 pb for $\alpha = 1.7$ and $\alpha = 1.5$, respectively. More concretely, for a c.m. energy of about 11.0 GeV and a parameter $\alpha = 1.7$ ($\alpha = 1.5$) as an example, the cross section is 0.70 (0.43) pb for $\bar{T}_{cc}^-$ production, which is accessible at the EICC [26] and US-EIC [27] due to the high luminosity of the future facilities. It is worth noting that, when we increase the c.m. energy to 50 GeV, which is far beyond the energy range of the planned EICC experiment, the cross section is also on the order of 1.0 pb. Thus, our results suggest that it will take at least one year of running at US-EIC to collect a hundred events.

As shown in Fig. 2, we present the variation of the total cross sections for different $\Gamma_{D^{*\pm} \to D^{\pm}\gamma}$ values, where $\Gamma_{D^{*\pm} \to D^{\pm}\gamma} = 0.979$–$1.704$ keV is taken from Ref. [1]. The results vary little and the cross section can reach 0.72 pb for

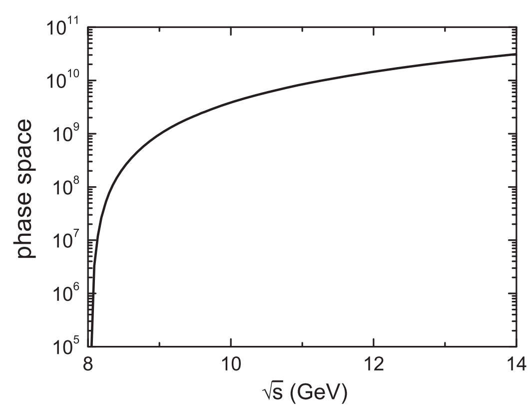

FIG. 3. The phase space for the $\gamma p \to D^+ \bar{T}_{cc}^- \Lambda_c^+$ reaction as a function of the center-of-mass energies.

the $\alpha = 1.7$ case at a c.m. energy of $\sqrt{s} = 11.0$ GeV, which should be compared with the central value of 0.7 pb.

Moreover, the coupling constants $g_{\Lambda_c pD}$ and $g_{D^* N\Lambda_c}$ are not firmly determined, and they will affect the estimated cross section. To see how much the cross section depends on the coupling constants $g_{\Lambda_c pD}$ and $g_{D^* N\Lambda_c}$, we show the cross section as a function of the c.m. energy in Fig. 4, where the coupling constants $g_{\Lambda_c pD}$ and $g_{D^* N\Lambda_c}$ are allowed to vary in reasonable ranges, i.e., $|g_{\Lambda_c pD}| = 10.7 \sim 13.98$ and $g_{D^* N\Lambda_c} = -(5.80 \sim 5.20)$. The values of $|g_{\Lambda_c pD}| = 10.7$, $g_{D^* N\Lambda_c} = -5.80$ [40,41] and $|g_{\Lambda_c pD}| = 13.98$, $g_{D^* N\Lambda_c} = -5.20$ [32,33] are obtained from the light-cone sum rules and SU(4) invariant Lagrangians in terms of $g_{\pi NN} = 13.45$ and $g_{\rho NN} = 6$ [34]. We find that the cross section is not very sensitive to the coupling constants. Taking the cross section at an energy of about $\sqrt{s} = 11.5$ GeV as an example, the so-obtained cross section ranges from 0.50 to 0.60 pb for $\alpha = 1.5$ and from 0.81 to 0.97 pb for $\alpha = 1.7$.

The individual contributions of Figs. 1(a) and 1(b) and the contact term for the $\gamma p \to D^+ \bar{T}_{cc}^- \Lambda_c^+$ reaction against the c.m. energy are shown in Fig. 5. From the figure, the contribution from Fig. 1(b) is a little larger than all the other contributions near the threshold. However, the contribution from the contact term becomes most important as the c.m. energy $\sqrt{s}$ increases from 9.3 to 12.0 GeV. We also notice that the interferences among them are sizable, leading to a bigger total cross section. The contribution from Fig. 1(a) is smaller than that from Fig. 1(b) near the threshold, whereas they become almost the same at high energies. A possible explanation is that the low-energy photon beam (still high to produce meson pairs) directly decaying to the charm meson pair $D^+ D^-$ is easier than that decaying to the $D^{*-} D^+$ pair [37,38,42–44].

Strictly speaking, such a high-energy interaction should employ the Regge approach to estimate the production cross section of T_{cc}^+ in the $\gamma p \to D^+ \bar{T}_{cc}^- \Lambda_c^+$ reaction, because the Regge approach is known to be able to explain very well high-energy scattering with unitarity preserved. Moreover, a unique feature of the Regge amplitudes is that

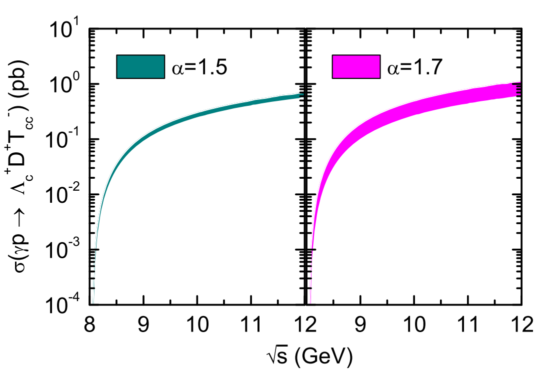

FIG. 4. Total cross section at the central value $g_{\gamma D D^*}$ for the $\gamma p \to D^+ \bar{T}_{cc}^- \Lambda_c^+$ reaction with $|g_{\Lambda_c pD}| = 10.7$–$13.98$ and $g_{D^* N\Lambda_c} = -5.80$–$-5.20$ [32,33,40,41] as a function of $\sqrt{s}$.

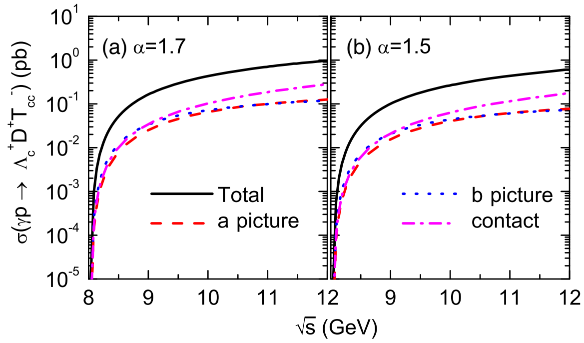

FIG. 5. Individual contributions of diagram a (red dashed line), diagram b (blue dotted line), and the contact term (magenta dash-dotted line) for the $\gamma p \to D^+ \bar{T}_{cc}^- \Lambda_c^+$ reaction as a function of the c.m. energy.

they can reproduce the diffractive pattern both at forward and backward scatterings as well as the asymptotic behavior consistently with unitarity. In other words, the Regge approach can be used to study the $\gamma p \to D^+ \bar{T}_{cc}^- \Lambda_c^+$ reaction via the current mechanism. The relevant Regge amplitudes for the charm mesons D and D^* exchange can be found in Ref. [45]. However, we found that even if the photon beam energy is very high, the energy transferred to the $\bar{D}$ and $\bar{D}^*$ meson to form the $\bar{T}_{cc}^-$ state is not much, accounting for about 8%–30% of the total energy. At this energy transfer, the total cross section is strongly suppressed from the $(s/s_0)^{\alpha_{D^{(*)}}}$ term and is on the order of 10^{-24} pb. It means that the Regge approach is not suited to study the production of $\bar{T}_{cc}^-$ in the $\gamma p \to D^+ \bar{T}_{cc}^- \Lambda_c^+$ reaction.

Finally, we should address the application scope of the current approach. Unfortunately, there is no information on the reaction studied, but one can estimate it from other reactions. The central diffractive mechanism has been widely employed to investigate hadron productions in pp collisions [22–25] in a large-energy range, especially the center-of-mass energy can reach and pass 100 GeV [23,24]. The experimental measurement can be well reproduced [22–25]. In addition, the cross section should not continuously increase with $\sqrt{s}$ at high energies as required by unitarity. We indeed find than the total cross section begins to decrease at a center-of-mass energy of about $\sqrt{s} = 500$ GeV [24] (see Fig. 7 in Ref. [24]) and the trend of the same decrease can also be found in our work at center-of-mass energies above 36.24 GeV. The results with $\alpha = 1.7$ are shown in Fig. 6. Thus, the current energy range we studied is appropriate.

IV. DISCUSSION AND SUMMARY

Inspired by the newly observed doubly charmed meson T_{cc}^+, we performed a detailed study of the nonresonant contribution to the $\gamma p \to D^+ \bar{T}_{cc}^- \Lambda_c^+$, to estimate the $\bar{T}_{cc}^-$ production rate at relatively high energies, where no data have been available up to now. The production process is described by the central diffractive and contact term, while

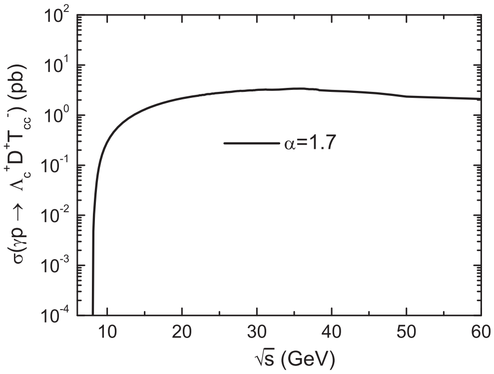

FIG. 6. Total cross section for the $\gamma p \to D^+ \bar{T}_{cc}^- \Lambda_c^+$ reaction with $\alpha = 1.7$ as a function of the center-of-mass energies.

the contributions for the $\gamma p \to D^+ \bar{T}_{cc}^- \Lambda_c^+$ reaction from $s-$ and $u-$ channels are ignored because the $s-$ and $u-$ channels that involve the creation of two additional $\bar{c}c$ quark pairs in the photon-induced production are usually strongly suppressed. The coupling constant of the $\bar{T}_{cc}^-$ to $\bar{D}^* \bar{D}$ is obtained from chiral unitary theory [18], where the $\bar{T}_{cc}^-$ is dynamically generated.

Our study showed that the cross section for the $\gamma p \to D^+ \bar{T}_{cc}^- \Lambda_c^+$ reaction can reach 1.0 pb. Although the photoproduction cross section is quite small, it is still possible to test our theoretical predictions thanks to the low background of the exclusive and specific reaction proposed in this work. The future electron-ion colliders of high luminosity in the U.S. (10^{34} cm^{-2} s^{-1}) [27,46] and China (2–4×10^{33} cm^{-2} s^{-1}) [26,47,48] provide a good platform for this purpose. For a year of running, around a hundred events can be collected. In experiment, it is vital to improve the detection efficiency of the multiple final-state particles of this reaction. To take advantage of the virtual photon of small virtuality on EIC, the far-forward electron detector is needed. The Roman pot frequently discussed could be used for this purpose. The photoproduction channel should be explored to study the exotic state T_{cc}^+ and its nature.

It is interesting to compare our results with those of Refs. [49,50]. In those works, they estimate the cross section by assuming T_{cc}^+ as a tetraquark. The production cross sections estimated in Ref. [50] can reach 10^4 pb at the LHC for $\sqrt{s} = 13$ TeV, which indicates that the LHCb detector might have already recorded such a state. This is quite different from our prediction. If the T_{cc}^+ state is measured and confirmed in future experiments, one is able to verify its nature by comparing the production cross sections predicted in different frameworks.

ACKNOWLEDGMENTS

This work was supported by the Science and Technology Research Program of Chongqing Municipal Education Commission (Grant No. KJQN201800510) and the Opened Fund of the State Key Laboratory on Integrated Optoelectronics (Grant No. IOSKL2017KF19). Y. H. is thankful for the support from the Development and Exchange Platform for the Theoretic Physics of Southwest Jiaotong University under Grants No. 11947404 and No. 12047576, the Fundamental Research Funds for the Central Universities (Grant No. 2682020CX70), and the National Natural Science Foundation of China under Grant No. 12005177.

[1] P. A. Zyla et al. (Particle Data Group), Prog. Theor. Exp. Phys. **2020**, 083C01 (2020).
[2] M. Gell-Mann, Phys. Lett. **8**, 214 (1964).
[3] N. Brambilla et al., Eur. Phys. J. C **71**, 1534 (2011).
[4] R. Aaij et al. (LHCb Collaboration), arXiv:2109.01038.
[5] R. Aaij et al. (LHCb Collaboration), Phys. Rev. Lett. **119**, 112001 (2017).
[6] N. Li, Z. F. Sun, X. Liu, and S. L. Zhu, Phys. Rev. D **88**, 114008 (2013).
[7] M. Z. Liu, T. W. Wu, M. Pavon Valderrama, J. J. Xie, and L. S. Geng, Phys. Rev. D **99**, 094018 (2019).
[8] R. Aaij et al. (LHCb Collaboration), arXiv:2109.01056.
[9] T. Mehen, Phys. Rev. D **96**, 094028 (2017).
[10] E. J. Eichten and C. Quigg, Phys. Rev. Lett. **119**, 202002 (2017).
[11] F. S. Navarra, M. Nielsen, and S. H. Lee, Phys. Lett. B **649**, 166 (2007).
[12] M. L. Du, W. Chen, X. L. Chen, and S. L. Zhu, Phys. Rev. D **87**, 014003 (2013).
[13] J. M. Dias, S. Narison, F. S. Navarra, M. Nielsen, J. M. Richard, S. Narison, and J. M. Richard, Phys. Lett. B **703**, 274 (2011).
[14] S. S. Agaev, K. Azizi, and H. Sundu, arXiv:2108.00188.
[15] L. Meng, G. J. Wang, B. Wang, and S. L. Zhu, Phys. Rev. D **104**, L051502 (2021).
[16] M. J. Yan and M. P. Valderrama, arXiv:2108.04785.
[17] X. K. Dong, F. K. Guo, and B. S. Zou, Commun. Theor. Phys. **73**, 125201 (2021).
[18] A. Feijoo, W. Liang, and E. Oset, Phys. Rev. D **104**, 114015 (2021).
[19] R. Chen, Q. Huang, X. Liu, and S. L. Zhu, arXiv:2108.01911.
[20] T. W. Wu, Y. W. Pan, M. Z. Liu, S. Q. Luo, X. Liu, and L. S. Geng, arXiv:2108.00923.

[21] X. Z. Ling, M. Z. Liu, L. S. Geng, E. Wang, and J. J. Xie, arXiv:2108.00947.
[22] P. Lebiedowicz and A. Szczurek, Phys. Rev. D **85**, 014026 (2012).
[23] P. Lebiedowicz, A. Szczurek, and R. Kaminski, Phys. Lett. B **680**, 459 (2009).
[24] P. Lebiedowicz and A. Szczurek, Phys. Rev. D **81**, 036003 (2010).
[25] A. B. Kaidalov, Phys. Rep. **50**, 157 (1979).
[26] D. P. Anderle, V. Bertone, X. Cao, L. Chang, N. Chang, G. Chen, X. Chen, Z. Chen, Z. Cui, L. Dai *et al.*, Front. Phys. (Beijing) **16**, 64701 (2021).
[27] A. Accardi, J. L. Albacete, M. Anselmino, N. Armesto, E. C. Aschenauer, A. Bacchetta, D. Boer, W. K. Brooks, T. Burton, N. B. Chang *et al.*, Eur. Phys. J. A **52**, 268 (2016).
[28] F. K. Guo, C. Hanhart, Y. S. Kalashnikova, U. G. Meißner, and A. V. Nefediev, Phys. Lett. B **742**, 394 (2015).
[29] F. K. Guo, C. Hanhart, U. G. Meißner, Q. Wang, Q. Zhao, and B. S. Zou, Rev. Mod. Phys. **90**, 015004 (2018).
[30] M. L. Du, V. Baru, F. K. Guo, C. Hanhart, U. G. Meißner, A. Nefediev, and I. Strakovsky, Eur. Phys. J. C **80**, 1053 (2020).
[31] Y. Huang, C. j. Xiao, Q. F. Lü, R. Wang, J. He, and L. Geng, Phys. Rev. D **97**, 094013 (2018).
[32] Y. Dong, A. Faessler, T. Gutsche, S. Kumano, and V. E. Lyubovitskij, Phys. Rev. D **82**, 034035 (2010).
[33] Y. Huang, J. He, J. J. Xie, and L. S. Geng, Phys. Rev. D **99**, 014045 (2019).
[34] S. Okubo, Phys. Rev. D **11**, 3261 (1975).
[35] D. Becirevic and B. Haas, Eur. Phys. J. C **71**, 1734 (2011).
[36] S. L. Zhu, W. Y. P. Hwang, and Z. s. Yang, Mod. Phys. Lett. A **12**, 3027 (1997).
[37] G. Pakhlova *et al.* (Belle Collaboration), Phys. Rev. D **77**, 011103 (2008).
[38] B. Aubert *et al.* (*BABAR* Collaboration), Phys. Rev. D **76**, 111105 (2007).
[39] X. D. Guo, D. Y. Chen, H. W. Ke, X. Liu, and X. Q. Li, Phys. Rev. D **93**, 054009 (2016).
[40] A. Khodjamirian, C. Klein, T. Mannel, and Y. M. Wang, Eur. Phys. J. A **48**, 31 (2012).
[41] A. Khodjamirian, C. Klein, T. Mannel, and Y. M. Wang, J. High Energy Phys. 09 (2011) 106.
[42] R. Poling (CLEO Collaboration), arXiv:hep-th/0606016.
[43] A. Osterheld *et al.* (Crystal Ball Collaboration), Report No. SLACPUB-4160, 1986.
[44] K. Abe *et al.* (Belle Collaboration), Phys. Rev. Lett. **98**, 082001 (2007).
[45] S. H. Kim, A. Hosaka, H. C. Kim, and H. Noumi, Phys. Rev. D **92**, 094021 (2015).
[46] R. Abdul Khalek, A. Accardi, J. Adam, D. Adamiak, W. Akers, M. Albaladejo, A. Al-bataineh, M. G. Alexeev, F. Ameli, P. Antonioli *et al.*, arXiv:2103.05419.
[47] X. Chen, Proc. Sci. DIS2018 (**2018**) 170.
[48] X. Chen, F. K. Guo, C. D. Roberts, and R. Wang, Few-Body Syst. **61**, 43 (2020).
[49] Y. Jin, S. Y. Li, Y. R. Liu, Q. Qin, Z. G. Si, and F. S. Yu, Phys. Rev. D **104**, 116008 (2021).
[50] Q. Qin, Y. F. Shen, and F. S. Yu, Chin. Phys. C **45**, 103106 (2021).